Available online at www.sciencedirect.com
SCIENCE DIRECT®
Journal of Power Sources 132 (2004) 302–308
JOURNAL OF POWER SOURCES
www.elsevier.com/locate/jpowsour

Effect of particle size on the electrode performance of MgNi hydrogen storage alloy

Carine Rongeat, Lionel Roué*

INRS-Énergie, Matériaux et Télécommunications, 1650 Boulevard Lionel Boulet, C.P. 1200, Varennes (Que.), Canada, J3X 1S2

Received 10 December 2003; accepted 28 December 2003

Abstract

Amorphous MgNi material has been synthesized by mechanical alloying and sieved into three particle size fractions: >75, 20–75, and <20 μm. The influence of the MgNi particle size on its electrochemical behavior as negative electrode for Ni–metal hydride (MH) batteries has been investigated. The initial discharge capacity is higher as the MgNi particle size increases, i.e. the initial discharge capacity of particles larger than 75 μm is 439 mAh/g compared to 396 and 328 mAh/g for 20–75 and <20 μm particles, respectively. In addition, the cycle life of the MgNi electrode is improved by increasing the particle size. That is, the >75 μm particles electrode retains 41% of its initial capacity after 15 cycles compared to 35 and 23% for 20–75 μm and <20 μm particles electrodes, respectively. The rate dischargeability is also improved by increasing the MgNi particle size. For example, at 400 mA/g, the >75 μm particles electrode delivers 33% of its capacity measured at 20 mA/g compared to 25 and 19% for 20–75 μm and <20 μm powders, respectively. These results can be explained by the lower specific surface area of the electrode constituted of large particles which limits the formation of $Mg(OH)_2$ resulting from the MgNi oxidation by the electrolyte. Moreover, on the basis of the evolution of the cycling discharge capacities with increasing charge input for the different powder fractions, it appears that the electrode resistance to pulverization is improved by increasing the MgNi particle size.

Keywords: Nickel–metal hydride battery; Hydrogen storage alloys; Magnesium-based compounds; Mechanical alloying

1. Introduction

Magnesium-based alloys exhibit promising properties as negative electrode material for Ni–metal hydride (MH) batteries. For example, amorphous MgNi obtained by mechanical alloying has an initial discharge capacity close to 500 mAh/g [1] compared to ∼300 mAh/g for $LaNi_5$-type alloys used in commercial Ni–MH batteries. Nevertheless, MgNi alloy is not satisfactory for practical use because of its rapid degradation during cycling in KOH electrolyte. Indeed, a capacity decay of 70% is observed after only 20 charge/discharge cycles [1]. This decay is related to the growth of a $Mg(OH)_2$ layer on the particles surface [2]. This layer consumes active material and may act as a barrier for charge transfer and hydrogen diffusion reactions. Moreover, due to the alloy expansion/contraction during charge/discharge cycles, powder pulverization occurs which creates new surfaces to be oxidized and then the electrode degradation is accelerated [3].

The performance of the metal hydride electrode depends greatly on the composition and the microstructure of the active material and consequently, the majority of the studies for improving the MH electrode performance are focused on this aspect. The charge and discharge conditions have also a major influence on the electrode performance. Finally, the electrode configuration including its porosity, its thickness, the concentration, and the nature of the additives and the particle size can also affect substantially the electrode performance.

Concerning the effect of particle size, several authors have reported its influence on the electrochemical properties of AB_5-type alloys [4–11]. For example, Boonstra et al. [4] showed that the activation process of an $LaNi_5$ electrode is faster as the $LaNi_5$ particle size decreases. They explain this result by the larger specific surface area of the powder constituted of small particles. Consequently, the current density at the surface of the small $LaNi_5$ particles is lower, which leads to more efficient charge and discharge processes, resulting in a higher amount of absorbed/desorbed hydrogen. This accentuates the powder pulverization and then the activation process is accelerated. In addition, due to the higher specific surface area of the powder constituted

* Corresponding author. Tel.: +1-450-929-8185; fax: +1-450-929-8102.
E-mail address: roue@inrs-emt.uquebec.ca (L. Roué).

0378-7753/$ – see front matter © 2004 Elsevier B.V. All rights reserved.
doi:10.1016/j.jpowsour.2003.12.049

of small particles, its oxidation by the electrolyte is accentuated and then its capacity degradation with cycling is more marked. In contrast, Naito et al. [5] showed that the maximum discharge capacity and the high-rate dischargeability of an $MmNi_{3.31}Mn_{0.37}Al_{0.28}Co_{0.64}$ electrode are improved by increasing the alloy particle size from 20–25 to 106–125 μm. They indicated that the key factor is the selection of a particle size comparable to the pore size of the porous nickel substrate in order to achieve adequate current collection. Notten et al. [6] compared the cycle life behavior of $LaNi_{4.4}Cu$ electrodes made from different particles size fraction. It appears clearly that the electrode surface area (related the particles size) is an important factor in determining the rate of oxidation and thus, the cycling stability of the electrode. However, the maximum discharge capacities of these electrodes are identical. Zhaoliang and Dongsheng [7] carried out comparative study of the performance of MmB_5 electrodes composed of particles with different sizes (from <30 to 74–147 μm). The electrode with 54–74 μm particles has the best discharge capacity, high-rate dischargeability and long-term stability. No particle size effect was observed on the activation process. Heikonen et al. [8] investigated the effect of particle size on the discharge performance of a Ni–MH cell with a mathematical model. A key parameter in this model is the conductivity of the solid phase which is mainly related to the particle-to-particle resistance. It must be noted that electrode pulverization as well as alloy oxidation are not considered in their model. It appears from the simulations that the particles size affects the electrode performance and this effect becomes more importance as the discharge rate increases. They showed that, for a given active surface area, better electrode performance can be achieved by using a nonuniform particle size. In addition, a simulated Ragone plot for different particle sizes [9] indicates that the energy density increases slightly due to the decrease in the particle size. A more important effect is observed on the electrode power density because a smaller particle reduces the time taken by hydrogen to reach the surface. Ise et al. [10] found that small particles are suitable to improve the MH electrode performance. However, too small particles (under 25 μm) decrease the discharge capacity and the cycle life because the contact resistance between the particles increases due to swelling of the electrode. The study of Yuan and Xu [11] on MmB_5 alloy with particle sizes varying from 125 to 25.5 μm showed that the smaller the particle size, the larger is the first discharge capacity and the earlier is the saturation capacity reached. On the other hand, the maximum discharge capacity increases with increasing particle size. The capacity decay with cycling is almost independent on the particle size except for the 25.5 μm particles which show a slightly faster decay rate.

According to these different studies, it is obvious that MH particle size is a key parameter for the elaboration of high-performance electrodes for Ni–MH batteries. However, several contradictory results have been highlighted and there is no consensus concerning the optimal MH particle size. Moreover, to our knowledge, no study has been reported about the influence of particle size on the performance of Mg-based materials. In this work, amorphous MgNi alloy was prepared by high energy ball milling and the effects of particle size on its electrochemical hydrogen storage properties were investigated.

2. Experimental details

Pure Mg (99.9%, chips) and Ni (99.9%, 100–200 mesh) in 1:1 atomic ratio were introduced with three steel balls (two with 11 mm diameter and one with 14 mm diameter) into a steel vial sealed under Argon atmosphere. The ball-to-powder mass ratio was 10:1. Mechanical alloying was performed for 10 h using a Spex 8000 vibratory mill. Several mills were performed in order to obtain a total mass of MgNi powder of about 20 g. The milled powder was separated by passing through sieves in three fractions: <20, 20–75, and >75 μm. The mass yield of these different particles size fractions was 26, 37, and 37%, respectively.

X-ray diffraction (XRD) analyses were performed using a Bruker D8 diffractometer with Cu Kα radiation. Scanning electron microscopy (SEM) observations were made using a Jeol JSM-6300F microscope operating at 15 kV.

Electrochemical charge/discharge tests were performed on an Arbin BT2000 battery tester at room temperature in 6 M KOH electrolyte using a three electrodes cell. The working electrode is composed of 100 mg of active material mixed with 800 mg of graphite and 20 mg of carbon black. The electrode was vacuum-impregnated with electrolyte for few minutes in order to have a completely wetted internal surface The counter electrode was a nickel wire and the reference electrode was an Hg/HgO electrode. In charge–discharge cycle tests, the working electrodes were charged at 200 mA/g for 3 h and discharged at 20 mA/g until −0.6 V versus Hg/HgO. For the high-rate dischargeability experiments, the procedure is similar except the discharge current density varying from 20 to 400 mA/g. The influence of the charge input was studied by varying the charge duration at 200 mA/g from 60 to 90 min with a discharge current density fixed at 20 mA/g until −0.6 V. In order to perform XRD analysis of the MH powders after cycling, working electrodes composed of 1 g of MgNi powder without carbon and graphite were used. These electrodes were charged/discharged 15 times under the cycle life test conditions described previously and then rinsed with water and dried at room temperature.

3. Results and discussion

3.1. Structural and morphological characterizations

XRD patterns for the three particles fractions are similar and correspond to the one obtained for as-milled MgNi,

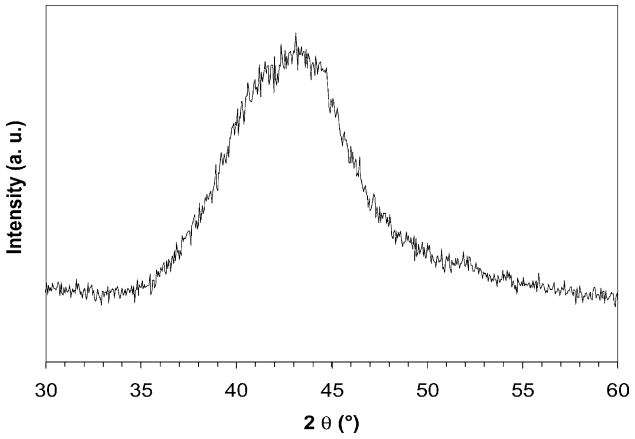

Fig. 1. XRD pattern of MgNi alloy obtained after 10 h of milling.

i.e. a broad peak centered around 42.5° characteristic of an amorphous structure (Fig. 1).

SEM observations of the three powder fractions of MgNi (Fig. 2) confirm the efficiency of the sieving procedure. Independently of their size, the particles present a very irregular shape with a marked roughness character. Particles are indeed an agglomeration of smaller ones which is the result of the repeated fracturing and cold welding processes involved in the mechanical alloying process [12]. EDX analyses reveal that magnesium and nickel are in similar proportions for the three particles fractions, in accordance with the nominal powder composition.

3.2. Electrochemical characteristics

3.2.1. Initial discharge capacity and cycle life

The discharge capacities with cycling for the three MgNi powder fractions are represented in Fig. 3. On the contrary to $LaNi_5$-type alloys, no activation period is observed during cycling: maximum discharge capacity is obtained at the first cycle and then the capacity decreases continuously with increasing cycle number. The activation phenomenon of $LaNi_5$-based materials is generally attributed to the powder pulverization which increases the effective surface area of the electrode. It can also be related to an improvement of the electrocatalytic properties of the electrode surface (i.e. increase of the electrochemical rate constant for the hydrogen charge transfer reaction) [6,13] through the rupture and/or dissolution of the native oxide layer covering the $LaNi_5$-based particles. Absence of activation period for MgNi electrodes does not preclude the powder cracking during cycling. This process accentuates greatly the MgNi oxidation and thus, decreases its discharge capacity instead of improving the electrode activity as observed for $LaNi_5$-based materials. This reflects the higher sensitivity of the MgNi powder to oxidation by the electrolyte in comparison to $LaNi_5$-based alloys.

From Fig. 3, it appears clearly that the initial discharge capacity is higher as the MgNi particle size increases: the initial discharge capacity of particles larger than 75 μm is 439 mAh/g compared to 396 and 328 mAh/g for 20–75 μm and <20 μm particles electrodes, respectively. This can be explained by the less serious oxidation for MgNi electrode constituted of large particles due to a lower surface area

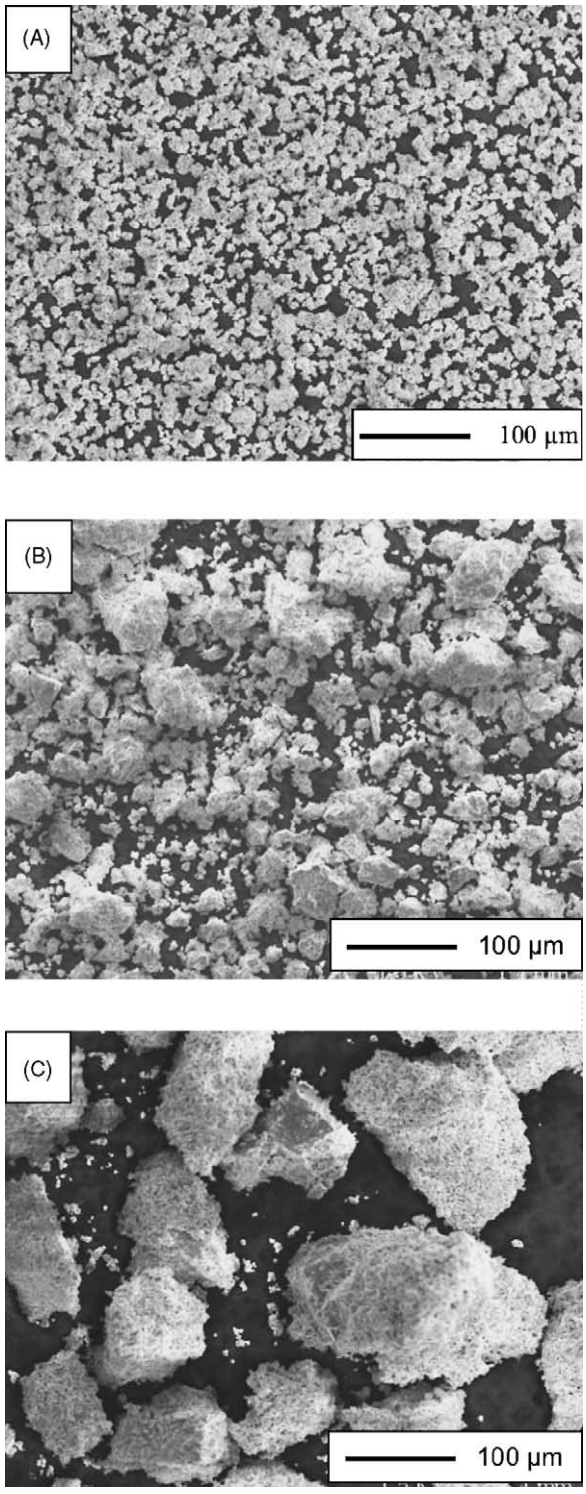

Fig. 2. SEM images of the MgNi powder fractions: (A) <20 μm, (B) 20–75 μm, and (C) >75 μm.

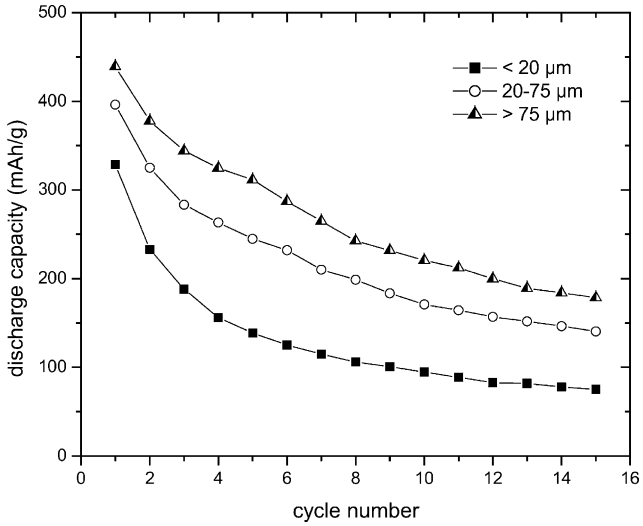

Fig. 3. Cycling discharge capacities of MgNi electrodes for different particle sizes.

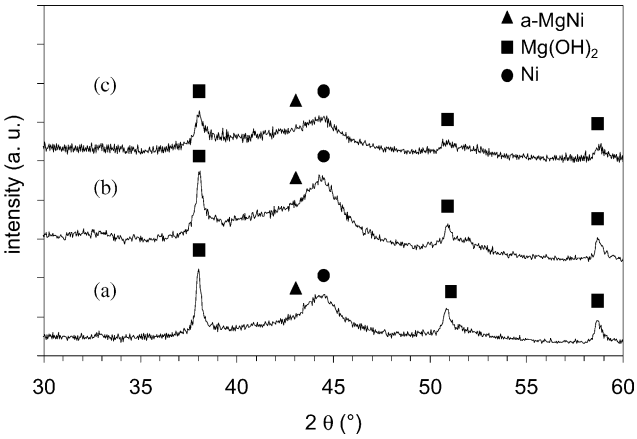

Fig. 4. XRD patterns after cycling for the three MgNi powder fractions: (a) <20 μm, (b) 20-75 μm, and (c) >75 μm

in contact with the electrolyte. For example, assuming that after immersion of the MgNi powder in KOH electrolyte, the thickness of the $Mg(OH)_2$ layer is 1 μm (a thickness range typically measured on Mg after immersion in aqueous media [14]), the fraction of unoxidized material is 92% for a 75 μm particle compared to 73% for a 20 μm particle. Thus, because electrode with larger particles has a more important fraction of active (i.e. no oxidized) MgNi material, it is not surprising that its initial discharge capacity is higher.

Fig. 3 also indicates that MgNi cycle life is improved by increasing the particle size. The >75 μm particles electrode retains 41% of its initial capacity after 15 cycles compared to 35 and 23% for 20–75 and <20 μm particles electrodes, respectively. The higher specific surface area of the electrode constituted of small particles accelerates its oxidation by the electrolyte and thus its capacity decay with cycling. In order to confirm this, XRD measurements have been carried out on electrodes after cycling for the three powder fractions (Fig. 4). After 15 charge/discharge cycles, new peaks attributed to $Mg(OH)_2$ and Ni appear on the XRD patterns. $Mg(OH)_2$ peaks become more apparent as the particles size decreases. This confirms that the electrode oxidation is accentuated with decreasing the particle size. This can be compared to the electrochemical behavior of $LaNi_5$-based powders indicating that the electrode surface area related to the particles size is an important factor in determining the oxidation rate and thus, the cycling stability of the MH electrode [6].

3.2.2. Particle pulverization

We have recently shown that the continuous discharge capacity decay of the MgNi electrode upon cycling can be prevented by controlling the electrode charge input [3]. It was demonstrated that capacity degradation during charge/discharge cycles is closely related to the electrode pulverization which is greatly accentuated when the charge input is higher than 233 mAh/g (i.e. $MgNiH_{0.7}$). For lower charge inputs, the volume expansion related to H absorption is assumed to be insufficient to induce a continuous pulverization of the MgNi particles upon cycling and thus, no capacity decay with cycling is observed. In other words, for charge inputs lower that 233 mAh/g, the passive $Mg(OH)_2$ surface layer formed onto the MgNi particles during the first cycle is not broken and therefore, it maintains its protective function against further corrosion.

In order to evaluate the influence of the particle size on the MgNi powder decrepitation, we have thus determined the charge input threshold inducing continuous capacity decay with cycling for the three particle size fractions. For that purpose, charge/discharge cycles were performed by increasing the charge input value from 200 to 300 mAh/g by step of 20 mAh/g. Five consecutive charge/discharge cycles were carried out for each charge input value. The results are presented in Fig. 5. For the three powder fractions, the initial discharge capacity is higher than the charge input. This additional discharge capacity can be associated with the MgNi oxidation into $Mg(OH)_2$ and $Ni(OH)_2$ during the discharge procedure [3]. This additional discharge capacity is lower for <20 μm particles than for larger particles (15 mAh/g for <20 μm particles compared to 50–55 mAh/g for 20–75 and >75 μm particles). This may reflect their more rapid oxidation, i.e. for small particles, a large part of the MgNi oxidation occurs during the charging procedure and then, the anodic charge related to their oxidation into $Mg(OH)_2$ and $Ni(OH)_2$ during discharge becomes less important.

As seen in Fig. 5, the discharge capacity decay does not appear at the same charge input value. For <20 μm particles, the discharge capacity decrease rapidly from the first cycle indicating that the charge input threshold is inferior to 200 mAh/g. Additional experiments with charge inputs varying from 100 to 200 mAh/g (not shown) reveal that the charge input value inducing electrode capacity degradation with cycling is 140 mAh/g for this powder fraction. For 20–75 μm particles, the capacity degradation is observed

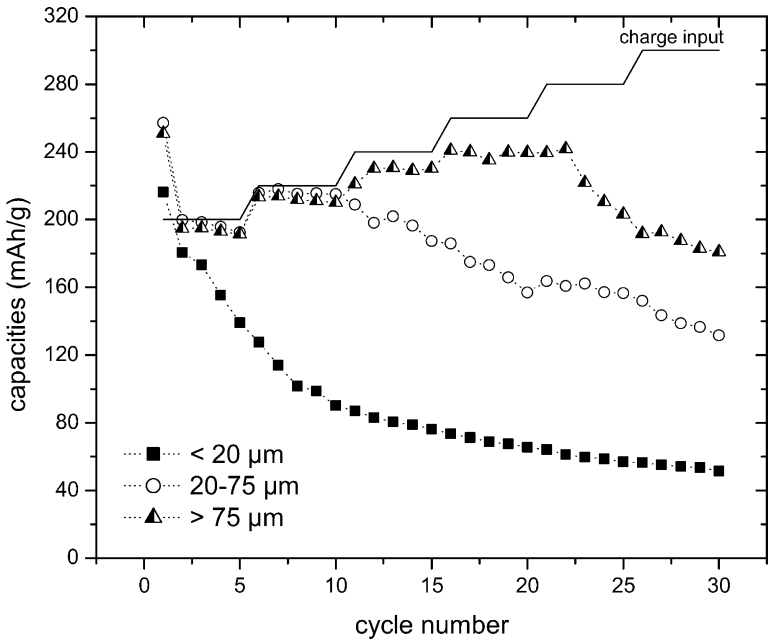

Fig. 5. Cycling discharge capacities with increasing charge input (solid line) of MgNi electrodes with different particle sizes.

for charge input higher than 220 mAh/g. For >75 μm particles, the charge input threshold is 260 mAh/g. In addition, an increasing difference between the charge input value and the discharge capacity appears as the charge input value increases. This may be attributed to a diminishing of the charge efficiency related to the hydrogen evolution side reaction which is favored with increasing charge input.

The fact that the charge input threshold inducing capacity degradation increases as the particle size increases may result from an increase of the proportion of active materials due to a decrease of the MgNi oxidation with increasing particles size as indicated previously. However, the ratios of the charge input threshold inducing continuous capacity degradation (from Fig. 5) to the maximum discharge capacity (from Fig. 3) are around 40, 55, and 60% for <20, 20–75, and >75 μm powder fractions, respectively. These values can be considered, in first approximation, as the maximum states of charge that the electrodes can support without continuous powder pulverization during cycling. The fact that this value raises with the particle size seems to indicate that the electrode resistance to pulverization increases as the MgNi particle size increases. It is surprising because the volume change induced by hydrogen absorption/desorption must be logically more important with large MgNi particles (due to the larger proportion of active material). It is also in contradiction with the study of Chung and Perng [15] indicating the difficulty to produce cracking by repeated hydriding–dehydriding for AB_5 particles smaller than 10 μm. In the present case, a possible explanation is that the smaller particles may have a larger internal strain due to a higher fraction of collision energy transferred to the powder when small particles are involved in impact events during the ball milling process. Consequently, their stress resistance related to the hydrogenation process would be diminished, leading to their pulverization from a lower hydrogen concentration. In order to confirm this hypothesis, the determination of the internal strain (from X-ray diffraction broadening) as a function of the particle size will be required. However, such a procedure is not possible due to the amorphous character of the MgNi powder. Another explanation is that the volume change induced by hydrogen charging/discharging is easier to relax with the large particles due to their larger proportion of void compared to the small particles presenting a more compact morphology.

Accurate quantification of MgNi powder pulverization through comparative BET surface area measurements before and after cycling is not possible. Indeed, the increase in surface area related to particle pulverization is overshadowed by the high surface area of $Mg(OH)_2$ formed onto the MgNi powder during cycling. Besides, gas phase hydrogen absorption/desorption cycles onto MgNi powder require high temperature (300 °C) leading to its crystallization and thus, the subsequent BET surface area measurements are also altered.

3.2.3. Rate dischargeability

The rate dischargeability of the three MgNi powder fractions for discharge current density varying from 20 to 400 mA/g is represented in Fig. 6. The rate dischargeability is denoted by the C^i/C^{20} ratio, in which C^i and C^{20} are the initial discharge capacity measured at the discharge current density of i and 20 mA/g, respectively. Independently of the MgNi particle size, the rate dischargeability of MgNi follows the same evolution, i.e. the electrode discharge capacity decreases as the discharge current density increases. This behavior is observed in most battery systems [16] and it is related to a shift of the discharge electrode potential and

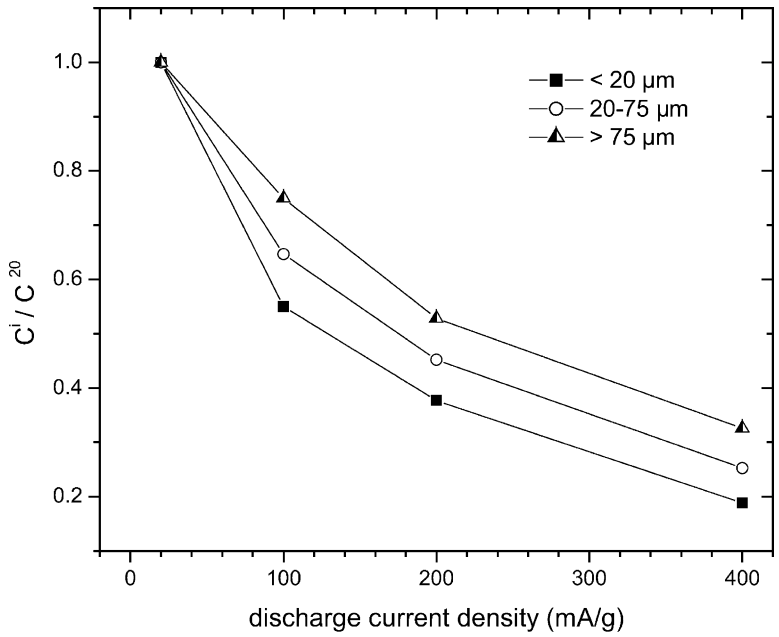

Fig. 6. Rate dischargeability of MgNi electrodes with different particle sizes.

a more marked slope of the discharge curve reducing the discharge time before the cut-off voltage. This is ascribed to an increase of the ohmic loss associated with the internal cell resistance and an increase of the charge-transfer and concentration polarizations with increasing current drain.

As seen in Fig. 6, the rate dischargeability is improved by increasing the MgNi particle size. For example, at 400 mA/g, the >75 μm particles electrode delivers 33% of its capacity measured at 20 mA/g compared to 25 and 19% for 20–75 and <20 μm particles electrodes, respectively. The more serious oxidation of the electrode containing smaller particles may explain this result. Indeed, the $Mg(OH)_2$ layer covering the MH particles must limit the electron transfer reaction and, in less extent, the hydrogen diffusion process, inducing an increase of charge-transfer and concentration overpotentials. Moreover, the presence of $Mg(OH)_2$ in large proportion at the surface of the MgNi particles may accentuate the ohmic resistance of the electrode due to a less efficient electron transfer between the MgNi particles and between the MgNi particles and the graphite used as current collector.

4. Conclusion

The electrochemical behavior of ball-milled MgNi used as negative electrode for Ni–MH batteries is significantly influenced by the MgNi powder size. The initial discharge capacity, the cycling stability and the high-rate dischargeability are improved by increasing the MgNi particle size. It seems to be related to a lower sensitivity to oxidation and to a better pulverization resistance of the electrode as the MgNi particle size increases. The next step will consist to couple the particle size effect with the modification of the MgNi composition. In addition, an optimization of the ball milling parameters favoring the powder coalescence process or an end-product agglomeration procedure will be required in order to increase the proportion of large Mg-based particles resulting from a milling.

Acknowledgements

This work has been financially supported by the National Sciences and Engineering Research Council (NSERC) of Canada and the “Fond de Recherche sur la Nature et les Technologies” of Québec.

References

[1] S. Ruggeri, C. Lenain, L. Roué, H. Alamdari, G. Liang, J. Huot, R. Schulz, Mat. Sci. Forum 377 (2001) 63.
[2] S. Ruggeri, L. Roué, J. Huot, R. Schulz, L. Aymard, J.M. Tarascon, J. Power Sources 112 (2002) 547.
[3] S. Ruggeri, L. Roué, J. Power Sources 117 (2003) 260.
[4] A.H. Boonstra, T.N. Bernards, G.J.M. Lippits, J. Less Common Metals 159 (1990) 327.
[5] K. Naito, T. Matsunami, K. Okuno, M. Matsuoka, C. Iwakura, J. Appl. Electrochem. 23 (1993) 1051.
[6] P.H.L. Notten, R.E.F. Einerhand, J.L.C. Daams, J. Alloys Comp. 210 (1994) 221.
[7] Z. Zhaoliang, S. Dongsheng, J. Alloys Comp. 270 (1998) L7.
[8] J.M. Heikonen, H.J. Ploehn, R.E. White, J. Electrochem. Soc. 145 (1998) 1840.
[9] G. Zheng, B.S. Haran, B.N. Popov, R.E. White, J. Appl. Electrochem. 29 (1999) 361.

[10] T. Ise, T. Murata, Y. Hirota, M. Nogami, S. Nakahori, J. Alloys Comp. 298 (2000) 310.
[11] X. Yuan, N. Xu, Int. J. Hydrogen Energy 26 (2001) 697.
[12] C. Suryanarayana, Prog. Mater. Science 46 (2001) 1.
[13] J.J.G. Willems, Philips J. Res. 39 (1984) 1.
[14] J.H. Nordlien, K. Nisancioglu, S. Ono, N. Masuko, J. Electrochem. Soc. 144 (1997) 461.
[15] S.R. Chung, T.P. Perng, J. Alloy Comp. 353 (2003) 289.
[16] D. Linden, T.B. Reddy (Eds.), in: Handbook of Batteries, third ed., McGraw-Hill Inc., New York, 2001.